Confining Barriers for Surface State Electrons Tailored by Monatomic Fe Rows on Vicinal Au(111) Surfaces

Susumu Shiraki,[1] Hideki Fujisawa,[1] Masashi Nantoh,[1,2] and Maki Kawai[1]

[1]*RIKEN (The Institute of Physical and Chemical Research), 2-1 Hirosawa, Wako, Saitama 351-0198, Japan*
[2]*"Organization and Function," PRESTO, Japan Science and Technology Corporation (JST), Saitama 332-0012, Japan*

We fabricated monatomic Fe wires on vicinal Au(111) surfaces and found that decoration of step edges with Fe adatoms has a significant influence on the behavior of surface state electrons confined between regularly arranged steps. On a surface with Fe monatomic rows, angle-resolved photoemission spectra measured in the direction perpendicular to the steps shows parabolic dispersion, in contrast to one-dimensional quantum-well levels observed on a clean surface. Simple analysis using a one-dimensional Kronig-Penney model reveals potential barrier reduction from 20 to 4.6 eV Å, suggesting an attractive nature of the Fe adatoms as scatterers.

Vicinal Au(111) surfaces have attracted considerable interest as suitable model systems to study electron wave functions [1–3]. The Au(111) surface provides a Shockley-type surface state, which behaves like a two-dimensional (2D) free-electron gas [4]. Since the surface state electrons scatter at step edges [5,6], the existence of highly regular step arrays leads to superlattice effects, electron confinement within terraces, and standing waves resulting in quasi-one-dimensional (1D) electronic structures. The strength of a 1D nature is dominated by the step potential barrier height $U_0 a$ to the surface state electrons. Recent angle-resolved photoemission spectroscopy (ARPES) studies revealed that, on the Au(322) surface (the step distance $L \sim 13$ Å), surface electrons propagate across the steps forming 2D superlattice bands [3]. On the other hand, on the Au(788) and the Au(23,23,21) surfaces ($L \sim 39$ and ~ 56 Å, respectively), quantum wells between adjacent steps confine surface electrons within terraces and form 1D quantum levels corresponding to standing waves in real space [1,2]. These results indicate that $U_0 a$ increases as L becomes larger, which is reasonably understood by using a 1D Kronig-Penney (KP) model [7–9].

Another unique utilization of the vicinal surfaces is high-quality natural templates for self-assembling of low-dimensional nanostructures such as ordered arrays of nanodots and nanowires [10]. Since step sites provide potential minima for adsorbates, regularly arranged steps induce a periodic change of the surface potential in the descending direction of the steps. Therefore, dosed atoms after diffusing around are trapped at potential minimum sites resulting in the formation of the structure having a 1D nature. On the vicinal Au(111) surfaces, so far, formation of an array of Co nanodots has been reported [11].

It has been suggested that the step potential barrier to the surface state electrons can be modified by decoration of the step edges with different species of atoms or molecules. Recently, Baumberger *et al.* reported that CO adsorption on vicinal Cu(111) surfaces reduces the potential barriers based on the observation of the energy shifts in photoemission dispersion plots [12]. However, studies on the vicinal surfaces with steps decorated with metal species are still lacking.

In this study, we fabricate Fe nanowires on the vicinal Au(111) surfaces and examine the surface electronic structures. Fe monatomic rows formed on the {111} steps are clearly observed by scanning tunneling microscopy (STM). Angular distributions of photoemission spectra are obtained by ARPES measurements before and after the formation of Fe nanowires. The influence of the step decoration with Fe on the surface state electrons confined within terraces is discussed in terms of the step potential barrier height estimated by using the 1D KP model.

As the vicinal Au(111) substrates, we employed Au(455) and Au(788) crystals. Rousset *et al.* studied the thermal behaviors of the vicinal Au(111) surfaces and found that Au(455) exhibits the hill-and-valley structure where both sides are vicinal facets with respective angles of 4° and 10° [13]. On the 4° phase, the reconstructed surface shows regularly spaced straight steps, so that we can easily distinguish dosed atoms by STM. Au(788) gives a vicinal facet with respective angle 3.5° [1], where the terrace width is slightly wider than the 4° phase. Since Au(788) shows equally spaced, straight monatomic steps on the entire sample region, the photoemission technique is available to obtain the information about the electronic band structure.

The substrates were stored in an ultra-high-vacuum chamber. The sample surface was prepared by extensive sputtering-annealing cycles until the LEED patterns displayed the characteristic spot splitting [13]. After cooling the sample to the room temperature (RT), Fe was deposited with an electron beam evaporator. The Fe flux was measured with a quartz-crystal film-thickness monitor. The typical deposition rate was 0.05 ML/min (ML is monolayer).

STM experiments were performed using a Beetle STM (Besocke Delta Phi GmbH) with an electrochemically etched W tip. All STM images were acquired in a constant current mode ($V_{tip} = +0.3$ V and $I = 0.5$ nA) at RT. ARPES experiments were carried out with an angle-resolved photoemission spectrometer (VG ADES 400) using He I radiation at RT.

STM observations with various Fe coverages have revealed the formation mechanism of the Fe nanowires. On the early stage of the formation, depressed spots and their aggregates are observed at step edges. These depressions are located with regular spacing at the fcc stacking regions of the surface reconstruction structure of Au(111) [14,15] and considered as Fe atoms substituted for Au at the step edge sites [16]. As the Fe coverage is increased, these exchange sites act as nucleation centers and create evenly spaced Fe fragments aligned along the steps, which are finally connected with each other forming the monatomic Fe rows. We discuss details about the growth mechanism elsewhere [17].

Figure 1 shows an STM image taken on the 4° phase of Au(455) at the Fe coverage of 0.04 ML. Atomically resolved Fe monatomic wires adsorbed at the lower corners of the {111} steps are clearly observed. This growth manner is in striking contrast to the nanodot formation with Co on the vicinal Au(111) surfaces [11], which seems to be strongly influenced by the surface reconstruction of the Au substrate [14,15]. It should be noted that the Fe wires do not form straight lines but show bumpy features. This reflects the fact that the Fe adatoms have two different adsorption sites depending on the species at the step edge (Au or substituted Fe) [17].

A recent ARPES study showed the quantum size effects on the vicinal Au(111) surfaces are considerably large compared with those on vicinal Cu(111) surfaces and can be observed at RT [1,2]. This is because the step potential barrier to the surface state electrons is so high that narrow terraces act as low-dimensional, electron-confining structures even at RT. As demonstrated by STM, however, dosed Fe atoms preferentially adsorb at the step edges and decorate them. Therefore, the step potential barrier is possibly modified by Fe adatoms, and behavior of the surface state electrons may change.

Figures 2(a) and 2(b) show the angular distributions of photoemission spectra measured in the direction perpendicular to the steps before and after the step decoration with Fe, respectively. The emission angle θ is measured with respect to the [788] surface normal direction. As marked with vertical bars in Fig. 2(a), two peaks with only a little dispersion are clearly observed on the clean Au surface. These discrete energy levels are described as the electronic states confined in quantum wells between slabs. The same observation was described in detail in a previous Letter [1].

At the Fe coverage of 0.04 ML, the spectra change strikingly as shown in Fig. 2(b). It is obvious that the peak near the Fermi level shows parabolic dispersion instead of the two peaks with little dispersion. This indicates that the electron propagation across the decorated steps on the vicinal surface is more free-electron-like and suggests that the step decoration with Fe decreases the potential barrier leading to a breakdown of the electron confinement. Figure 2(b) also shows a downward energy shift of the surface state band bottom compared to Fig. 2(a). The binding energies of the bottom are found
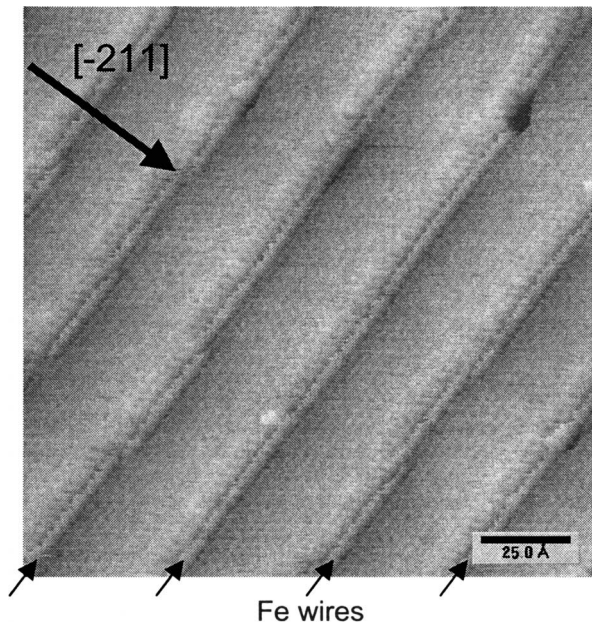

FIG. 1. One-dimensional Fe nanostructure grown on the Au(455) surface (0.04 ML). The surface is misoriented by 4° with respect to the Au(111) surface toward the $[-211]$ azimuth. The large arrow indicates the descending direction of the steps.
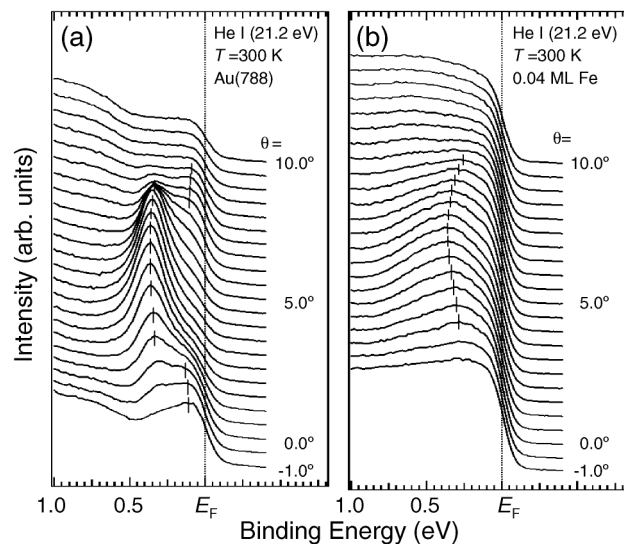

FIG. 2. Angular distributions of photoemission spectra near the Fermi level measured in the direction perpendicular to the step array: (a) Au(788) and (b) 0.04 ML Fe/Au(788). The emission angle θ is measured with respect to the surface normal.

at $E_b = 0.38$ and 0.40 eV in Figs. 2(a) and 2(b), respectively; thus we obtained the peak shift to the lower energy of 0.02 eV.

The 1D KP model [7–9] seems to be suitable for explaining the behavior of the surface state electrons on vicinal (111) surfaces of noble metals because of the 2D nature of the Shockley state [4] and the periodic potential induced by the regularly spaced steps. Actually, it has been used to discuss ARPES and scanning tunneling spectroscopy (STS) data measured on Cu [9,12] and Au [1–3,8]. However, it should be noted that this model neglects the coupling between the surface state and the bulk states. Therefore, if the probability of scattering into the bulk states (absorption) is not small, this model cannot describe the observing system adequately. Hörmandinger and Pendry investigated the behavior of periodic arrays of adatom rows as 1D scattering objects on Cu(111) employing the layer-Korringa-Kohn-Rostoker method [18]. They found that transition metals do not couple strongly to the bulk. They also pointed out that the probability of absorption increases if Bragg scattering increases the number of states into which the surface state electrons can scatter. Figure 1 shows nearly close-packed Fe adatom rows, which excludes this possibility. These facts give certain applicability of the 1D KP model to the system we observe.

Using the 1D KP model, the dispersion relation on the vicinal surface is described as

$$E(k) = \frac{\hbar^2}{2m^*L^2}[\cos^{-1}(|T|\cos kL) - \phi]^2, \quad (1)$$

where m^* is the effective mass of the surface state electrons, $T = |T|e^{i\phi}$ is the energy-dependent transmission coefficient through the step barriers, and the phase shift ϕ is the change in phase of the transmitted wave relative to the incident one. T is related to the step potential barrier U_0a and the surface state energies E by $T = q/(q + iq_0)$, where $q = \sqrt{2m^*E}/\hbar$ and $q_0 = m^*U_0a/\hbar^2$. The relation of Eq. (1) has two consequences: the upward energy shift of the bottom of the surface state band, and the opening of minigaps at $k = n\pi/L$, where $n = \pm1, \pm2, \cdots$, k is the wave vector perpendicular to the steps, and L is the terrace width [7–9]. As we will see, the downward energy shift observed in Fig. 2(b) is consistent with the dispersive feature of the spectra, suggesting that the Fe decoration of step sites makes the barrier less repulsive.

As can be seen in Fig. 2(a), two quantum levels slightly disperse and have finite subband widths, indicating that the electron confinement is not perfect. The step potential barrier height can be obtained by fitting the curvature of Eq. (1) to the data. In Fig. 3(a), the intensity of the spectra in Fig. 2(a) is demonstrated as a function of the kinetic energy and the wave number in gray scale, and a calculated curve is superimposed. For Au(788), $L = 39$ Å and $m^* = 0.28m_e$ are used. We obtain the step potential barrier height of 20 eV Å for Au(788). This value is relatively

higher than those found in other vicinal surfaces [2,3,9] but close to the value previously reported on Au(788) [1]. This fitting procedure also gives the bottom energy of the surface state band for the flat Au(111) surface of -0.45 eV below the Fermi level. Using this value, a calculated curve (dashed line) is fitted to the data obtained on 0.04 ML Fe/Au(788) (filled circles) in Fig. 3(b). We obtain U_0a for 0.04 ML Fe/Au(788) of 4.6 eV Å, indicating considerable reduction of the potential barrier by the step decoration with Fe.

Since $k = 0$ at the bottom of the dispersion relation of Eq. (1), the upward energy shift of the bottom relative to the surface state band on the flat (111) surface is given by

$$\Delta E = \frac{\hbar^2}{2m^*L^2}[\cos^{-1}(|T|) - \phi]^2. \quad (2)$$

Using this equation, Sánchez et al. estimated the step potential barriers on several vicinal Cu(111) surfaces [9]. In Fig. 4, ΔE (solid line) and the transmission probability $|T|^2$ (dashed line) for the electrons at the band bottom are plotted as a function of U_0a. When $U_0a = 0$ eV Å, $\Delta E = 0$ meV, $|T|^2 = 1.0$, and $\phi = 0$, corresponding to the free-electron-like behavior of the surface state electrons on the flat Au(111) surface. As U_0a increases, $|T|^2$ and ϕ decrease toward zero and $-\pi/2$, respectively, and ΔE increases toward 88 meV ($= \pi^2\hbar^2/2m^*L^2$). It is concluded from Fig. 4 that 0.04 ML Fe decoration on Au(788) decreases ΔE from 77 to 53 meV and increases $|T|^2$ from 0.01 to 0.12. Therefore, although the parabolic dispersion in Fig. 2(b) indicates the electron propagation across the steps, most of the surface state electrons are still strongly reflected by the steps (or absorbed by the bulk).

Hörmandinger and Pendry found that the transition and noble metal adatoms on Cu(111) act as attractive
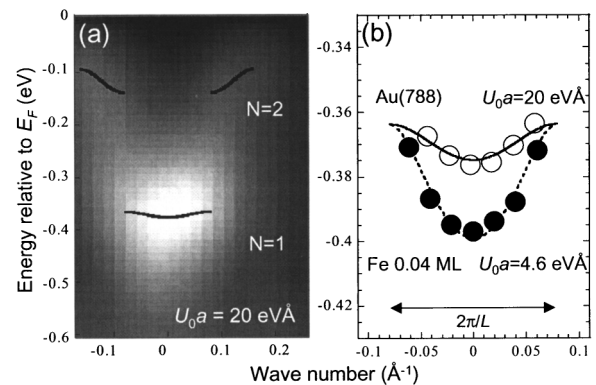

FIG. 3. Experimental band dispersion measured in the perpendicular direction to the step array and calculated curves using a 1D Kronig-Penney model. (a) The dispersion on the clean Au(788) surface (gray scale plots) and calculated curves (black lines) using $L = 0.39$ nm and $m^* = 0.28m_e$. (b) The data obtained from the peak positions in Fig. 2 (plotted by circles), and the calculated curves superimposed within the first Brillouin zone.
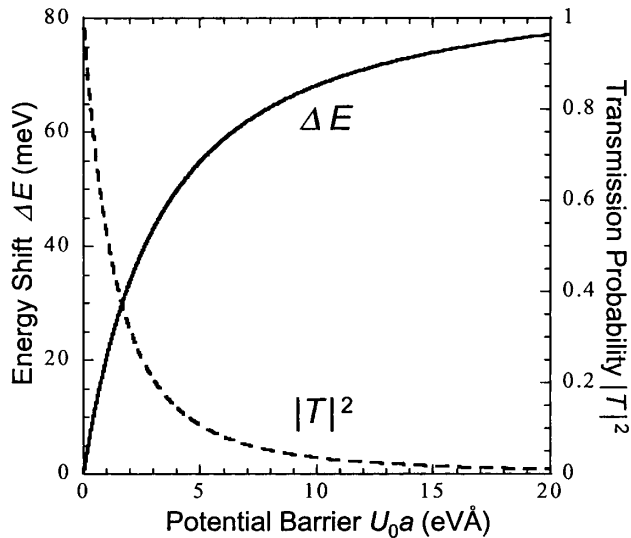
FIG. 4.   Upward energy shift of the surface state band bottom (solid line) and transmission probability across the barrier (dashed line) as a function of the potential barrier height at the steps.

scatterers of electrons, while p elements like sulfur and carbon are strongly repulsive scatterers [18]. Furthermore, Baumberger et al. recently found that even a repulsive scatterer can act as an attractive one on vicinal surfaces [12]. They decorated vicinal Cu(111) surfaces with CO molecules, which are regarded as repulsive scatterers on the flat Cu(111) surface and observed downward energy shifts of the band bottom indicating the attractive nature of the CO molecules at the step edges. These facts seem to give a plausible explanation for our result that the Fe adatom rows attached to the Au step edges tend to behave as attractive scatterers.

The attractive nature of the decorated steps can be attributed to the charge transfer from the step atoms to the adsorbates [12]. In the present case, the possible origin of such charge transfer may be the Friedel oscillation [19]. Kesmodel and Falicov obtained an approximate solution of the Shrödinger-Poisson-Hartree equation for a 90° metallic wedge and found that the Friedel oscillation is sizably enhanced near the steps because of the discontinuity [20]. Hasegawa and Avouris obtained energy dispersion of the surface state on Au(111) based on the STS data reflecting the standing waves near the steps, which was different from the dispersion obtained in previous ARPES experiments [21]. They concluded that this difference can be reasonably explained if the potential near the steps has a modulated component $\sim \cos(2k_F x)$ owing to the Friedel oscillation. If we regard the Fe adatom rows epitaxially grown on the Au {111} steps as parts of step edges, the first enhanced peak of the electron density of the oscillation must be located near the Fe rows, and charge transfer from Au to Fe must occur for the supplement. Since Fe has $3d$ bands with narrow widths, which is probably enhanced by the low-dimensional structure hav-

ing a small coordination number, the Fe rows have much larger density of states near the Fermi level than Au. Therefore, the charge transfer from Au to Fe could be a considerable effect even if the oscillation of the local potential is small.

Another possibility is that the substituted Fe atoms at the step edges cause the reduction of the potential barrier. The substitution can affect and perturb the local electronic structure near the step and possibly destroy the two dimensionality of the surface state electrons. This probably can reduce the reflection of the electrons at the step barrier and lead to the breakdown of the electron confinement.

Finally, we give further information about the electronic structures of Fe nanostructures formed on vicinal Au(111). We have measured photoemission spectra on Fe/Au(788) over a wide range of Fe coverages and have mapped out the band dispersion in the directions perpendicular and parallel to the steps. We found that the $3d$ bands of the Fe nanostructures show 1D electronic features at the coverages lower than ~0.6 ML, which seems to be reinforced by the quasi-1D electronic nature of the vicinal Au(111) substrate. We will report these ARPES results in the forthcoming papers.

[1] A. Mugarza et al., Phys. Rev. Lett. **87**, 107601 (2001).
[2] A. Mugarza et al., Phys. Rev. B **66**, 245419 (2002).
[3] J. E. Ortega et al., Phys. Rev. B **65**, 165413 (2002).
[4] W. Shockley, Phys. Rev. **56**, 317 (1939).
[5] M. P. Everson, R. C. Jaklevic, and W. Shen, J. Vac. Sci. Technol. A **8**, 3662 (1990).
[6] Ph. Avouris and I.-W. Lyo, Science **264**, 942 (1994).
[7] R. de L. Kronig and W. G. Penney, Proc. R. Soc. London A **130**, 499 (1931).
[8] L. C. Davis et al., Phys. Rev. B **43**, 3821 (1991).
[9] O. Sánchez et al., Phys. Rev. B **52**, 7894 (1995).
[10] F. J. Himpsel et al., Adv. Phys. **47**, 511 (1998), and references therein.
[11] V. Repain et al., Surf. Sci. **447**, L152 (2000).
[12] F. Baumberger et al., Phys. Rev. Lett. **88**, 237601 (2002).
[13] S. Rousset et al., Surf. Sci. **422**, 33 (1999).
[14] W. Chen et al., Phys. Rev. Lett. **80**, 1469 (1998).
[15] V. Repain et al., Appl. Surf. Sci. **162–163**, 30 (2000).
[16] J. A. Meyer et al., Surf. Sci. **365**, L647 (1996).
[17] S. Shiraki, H. Fujisawa, M. Nantoh, and M. Kawai (unpublished).
[18] G. Hörmandinger and J. B. Pendry, Phys. Rev. B **50**, 18 607 (1994).
[19] J. Friedel, Nuovo Cimento Suppl. **7**, 287 (1958).
[20] L. L. Kesmodel and L. M. Falicov, Solid State Commun. **16**, 1201 (1975).
[21] Y. Hasegawa and Ph. Avouris, Phys. Rev. Lett. **71**, 1071 (1993).